

OFFICE OF NAVAL RESEARCH

GRANT or CONTRACT: N00014-91-J-1919

96PRO-2855
Robert Nowak

Technical Report No. 23

In Situ STM and UHV-EC: Complementary,
not Competing, Techniques

Manuel P. Soriaga, Kingo Itaya, and John L. Stickney

submitted to

IUPAC Monograph "In Situ Local Probe Techniques
for Studies of Electrochemical Interfaces

Department of Chemistry
University of Georgia
Athens, GA 30602-2556

10/15/96

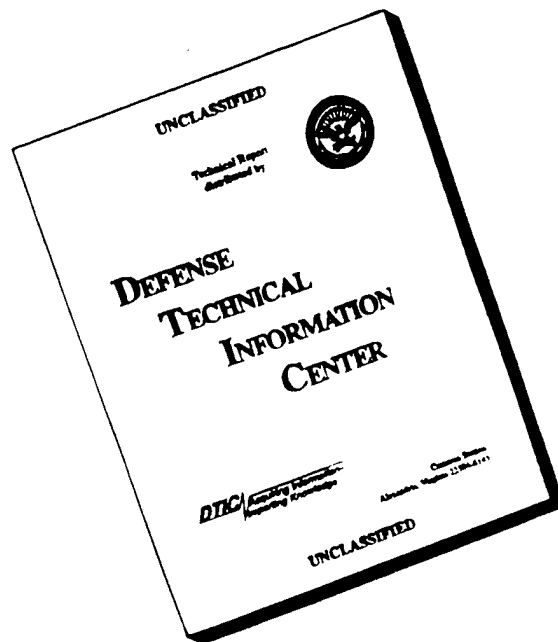
Reproduction in whole, or in part, is permitted for any purpose of the United States Government.

This document has been approved for public release and sale;
its distribution is unlimited.

DTIC QUALITY INSPECTED 3

19961030 106

DISCLAIMER NOTICE



THIS DOCUMENT IS BEST QUALITY AVAILABLE. THE COPY FURNISHED TO DTIC CONTAINED A SIGNIFICANT NUMBER OF PAGES WHICH DO NOT REPRODUCE LEGIBLY.

REPORT DOCUMENTATION PAGE			Form Approved OMB No. 0704-0188	
<small>Public reporting burden for this collection of information is estimated to average 1 hour per response, including the time for reviewing instructions, searching existing data sources, gathering and maintaining the data needed, and completing and reviewing the collection of information. Send comments regarding this burden estimate or any other aspect of this collection of information, including suggestions for reducing this burden, to Washington Headquarters Services, Directorate for Information Operations and Reports, 1215 Jefferson Davis Highway, Suite 1204, Arlington, VA 22202-4302, and to the Office of Management and Budget, Paperwork Reduction Project (0704-0188), Washington, DC 20503</small>				
1. AGENCY USE ONLY (Leave blank)		2. REPORT DATE 10/15/96		3. REPORT TYPE AND DATES COVERED Technical 6/1/95 - 10/15/96
4. TITLE AND SUBTITLE In Situ STM and UHV-EC: Complementary, not Competing, Techniques			5. FUNDING NUMBERS G-N00014-19-J-1919 Dr. Robert J. Nowak 96PRO-2855	
6. AUTHOR(S) Manuel P. Soriaga, Kingo Itaya and John L. Stickney				
7. PERFORMING ORGANIZATION NAME(S) AND ADDRESS(ES) John L. Stickney Department of Chemistry University of Georgia Athens, GA 30602-2556			8. PERFORMING ORGANIZATION REPORT NUMBER Technical Report #23	
9. SPONSORING/MONITORING AGENCY NAME(S) AND ADDRESS(ES) Office of Naval Research Chemistry Division 800 North Quincy Street Arlington, VA 22217-5660			10. SPONSORING/MONITORING AGENCY REPORT NUMBER	
11. SUPPLEMENTARY NOTES				
12a. DISTRIBUTION/AVAILABILITY STATEMENT Approved for public release and sale; its distribution is unlimited			12b. DISTRIBUTION CODE	
13. ABSTRACT (Maximum 200 words) <p>The development of <i>in situ</i> scanning tunneling microscopy (STM) has opened new avenues of research in electrochemical surface science. By itself, this nanometerscale structural tool cannot be regarded as a panacea for the many problems that confront researchers in the interfacial sciences. However, when employed in tandem with other surface-sensitive analytical methods, even exceedingly complex processes can be investigated. Two cases are presented here that showcase the power of <i>in situ</i> STM coupled with combined ultrahigh vacuum-electrochemistry (UHV-EC) techniques.</p>				
14. SUBJECT TERMS STM, in situ, UHV-EC, Pd, I, Se, Au			15. NUMBER OF PAGES 14	
			16. PRICE CODE	
17. SECURITY CLASSIFICATION OF REPORT Unclassified	18. SECURITY CLASSIFICATION OF THIS PAGE Unclassified	19. SECURITY CLASSIFICATION OF ABSTRACT Unclassified	20. LIMITATION OF ABSTRACT UL	

"In Situ Local Probe Techniques for Studies of Electrochemical Interfaces"

W. Plieth and W. Lorenz

Editors

IN SITU STM AND UHV-EC:
COMPLEMENTARY, NOT COMPETITING, TECHNIQUES

MANUEL P. SORIAGA

Department of Chemistry

Texas A&M University

College Station, TX 77843 USA

KINGO ITAYA

Department of Molecular Chemistry and Engineering

Faculty of Engineering

Tohoku University

Sendai 980, Japan

JOHN L. STICKNEY

Department of Chemistry

University of Georgia

Athens, GA 30602 USA

ABSTRACT

The development of *in situ* scanning tunneling microscopy (STM) has opened new avenues of research in electrochemical surface science. By itself, this nanometer-scale structural tool cannot be regarded as a panacea for the many problems that confront researchers in the interfacial sciences. However, when employed in tandem with other surface-sensitive analytical methods, even exceedingly complex processes can be investigated. Two cases are presented here that showcase the power of *in situ* STM coupled with combined ultrahigh vacuum-electrochemistry (UHV-EC) techniques.

INTRODUCTION

The invention of the scanning tunneling microscope (STM) [1] and the developmental work [2] that ensued to adapt the technique in the study of the electrode-electrolyte interface *under reaction conditions*, have provided significant advances in the area of electrochemical surface science. While such advances may tempt a few to regard the combination of STM and electrochemistry (STM-EC) as the panacea to the myriad problems in interfacial electrochemical science, it need only be stated that the utter complexity of heterogeneous processes cannot be unraveled by just one technique. The true strength of STM-EC lies in its integration with other surface-sensitive analytical methods such as those that permit the determination of other critical interfacial parameters such as composition and electronic structure; one such approach is the combination of STM-EC with tandem ultrahigh vacuum-electrochemistry (UHV-EC) [3].

In this paper, two studies are presented to showcase the power of UHV-STM-EC. The first illustration involves the dissolution of Pd that occurs only when a monolayer of iodine was present on the surface [4]. The structural features of the halogen-metal interface that accompany the adsorbate-catalyzed corrosion were first explored with low-energy electron diffraction (LEED); initial- and final-state structures were readily determined. However, questions, such as the mechanism for dissolution, required an *in situ* technique for answers; it was in this regard that STM-EC work was pursued [5].

The second example involves the surface chemistry of the compound semiconductor CdSe synthesized epitaxially on Au(100) by underpotential deposition (UPD). By analogy with the gas-phase epitaxial deposition procedure, this UPD-based method has been dubbed electrochemical atomic layer epitaxy (ECALE) [6]. Unique information on the interfacial structure of the first adlayer of Se electrodeposited was revealed upon STM experiments.

EXPERIMENTAL

The experimental procedures unique to the UHV-EC [4,6] and STM-EC [5] investigations have been described in detail elsewhere. UHV-EC work with Pd employed a commercially oriented and metallographically polished, 99.9999%-pure Pd(111) single-crystal electrode; STM-EC studies were done with Pd(111) single-crystal surfaces prepared by the Clavilier method, originally developed for Pt(111) surfaces [7]. For the ECALE work, an oriented and polished Au single crystal electrode was employed. Commercial instruments were used in the UHV-EC (Perkin-Elmer, Eden Prairie, MN) and STM-EC (Digital Instruments, Santa Barbara, CA) investigations.

RESULTS AND DISCUSSION

Adsorbate-catalyzed dissolution: Pd(111)-($\sqrt{3}\times\sqrt{3}$)R30°-I

Figure 1 shows the current-potential curve for a clean and an iodine-coated Pd(111) facet, formed on a single-crystal bead, in halide-free 0.05 M H₂SO₄. The exceedingly large anodic peak at about 1.2 V represents the Pd_(s)⁰-to-Pd²⁺_(aq) anodic stripping that occurs only when interfacial iodine is present [4,5]. It is important to mention that, if the potential is held just below 1.2 V, the current, as expected from a material-limited dissolution process, does not decay but remains constant.

Figure 2 shows photographs of LEED patterns for Pd(111)-($\sqrt{3}\times\sqrt{3}$)R30°-I prior to and after removal of about 30 monolayers of Pd surface atoms. In this experiment, the potential was held close to but not past the anodic dissolution peak; *that is, the dissolution was carried out at a fairly high rate*. The LEED data clearly show that the post-corrosion I-coated Pd surfaces remained as well-ordered as they were prior to the dissolution reaction. A layer-by-layer dissolution process is thus suggested. The LEED results, however, do not provide information on the corrosion transpires at steps or via place-exchange between the I and Pd atoms. For such information, *in situ* STM experiments were invoked.

Figure 3 shows typical STM-EC images of Pd(111)-($\sqrt{3}\times\sqrt{3}$)R30°-I before and after

the I-catalyzed dissolution; Figure 4 provides evidence for the well-ordered Pd(111)-($\sqrt{3}\times\sqrt{3}$)R30°-I structure at the terrace. In this experiment, a scratch on the surface was made to serve as a marker (M) and ensure that the STM scans are always done at the same area of the corroded surface. The top photograph was obtained prior to dissolution; the step, monatomic and diatomic in height, that was monitored during the dissolution process is marked S. The middle photograph was taken after 10 minutes of mild oxidative dissolution at 0.9 V, a potential at the foot of the anodic stripping peak. In this image, it can be seen that: (i) the step has moved towards the marker, and (ii) an enlarged smooth terrace has been formed. The bottom image was obtained after another 10 minutes of additional dissolution. It is more evident here that not only has the step progressed further towards the marker but also that the area of the atomically smooth terrace has become much larger. The formation of wide-area smooth terraces is in agreement with the sharp LEED patterns shown in Figure 3 after dissolution of multilayers of Pd surface atoms. The STM images in Figure 4 clearly demonstrate: (i) layer-by-layer dissolution, and (ii) selective corrosion at the steps, *at least under the present conditions of mild dissolution*.

It is difficult to obtain reliable STM-EC information at high dissolution rates; hence, the dissolution mechanism near the anodic peak has not been determined. As noted earlier, LEED experiments were carried out near the anodic peak; the possibility exists that place-exchange between the iodine and Pd interfacial atoms may transpire at such high dissolution rates yet result in an ordered final state upon emersion.

The STM result that dissolution of Pd atoms occurs selectively at step (disordered) sites provided the impetus for an additional study which demonstrated that the $I_{(ads)}$ -catalyzed anodic dissolution process is able to regenerate an ordered Pd(111) surface from one that had been subjected to extensive Ar^+ -ion bombardment [8]. This particular reordering reaction is unique because it occurs (i) in the absence of bulk corrosive reagent, and (ii) only if a chemisorbed layer of iodine is present. This process may be viewed similarly to digital etching [9] under electrochemical conditions

[10] except that (a) bulk material is not needed to replenish the adsorbed iodine that activates the surface, and (b) the dissolution process does not cease even after the atomically smooth surface has been regenerated.

Electrochemical Atomic Layer Epitaxy: Se on Au(100)

In the formation of the compound semiconductor CdSe on Au(100) by ECALE [6], the chalcogenide is the choice for the first atomic layer due to its increased stability after loss of potential control. If Cd is deposited first, it undergoes partial but spontaneous oxidation by residual oxygen gas; in the presence of a Se adlayer, no such Cd oxidation occurs as it is now stabilized by compound formation with Se.

On Au(100), Se is cathodically deposited, from a HSeO_3^- solution, in different atomic layer structures depending upon the duration and potential of electrodeposition. The structures formed were: Au(100)-p(2×2)-Se at a coverage Θ (\equiv Se atoms/Au atoms) of 0.2, Au(100)-(2×√10)-Se at $\Theta = 0.3$, Au(100)-c(2×2)-Se at $\Theta = 0.5$, and Au(100)-(3×√10)-Se at $\Theta = 0.9$ [6]. The LEED patterns for the Au(100)-c(2×2)-Se and Au(100)-(2×√10)-Se and adlattices are shown in Figures 4(A) and 4(B), respectively.

While the two-dimensional adlayer symmetries can quite readily be deduced from the LEED patterns, no information can be obtained on the chemical nature of the adlayer unless dynamical LEED simulations are performed [11]. The inclusion of STM in the arsenal of surface structural tools often negate the requirement of such LEED simulations. This is clearly illustrated in Figures 5(A) and 5(B) which, respectively, show the evolution of Se_8 rings as the coverage is increased from just above 0.5 to 0.9.

Coincident with the development of the Se_8 rings, was the formation on the surface of pits, a *random* occurrence that can be revealed only by STM experiments. Quantitative analysis of the STM images suggested that the pits (i) were monatomic in depth and, (ii) contained the same Se_8 ring structure on the bottom. The coverage of the pits accounts for about 10% of the total surface area at high Se coverages. Pit formation is discussed in greater detail elsewhere [6].

OUTLOOK

Among the many advantages of STM, two are most prominent in the cases described here: (i) its adaptability for measurements *under reaction conditions*, and (ii) its ability to resolve localized nanometer-scale structural features. Based upon these two advantages alone, it is not difficult to comprehend why STM has already become a pillar among the many powerful techniques employed in surface science. On the other hand, its inability to probe surface energetics, composition, and electronic structure, will always require additional surface spectroscopic techniques if a more complete understanding of complex heterogeneous processes is desired. A strategy that combines *in situ* STM with UHV-EC may be compelling since it bridges the gaps inherent in the separate techniques.

ACKNOWLEDGMENTS

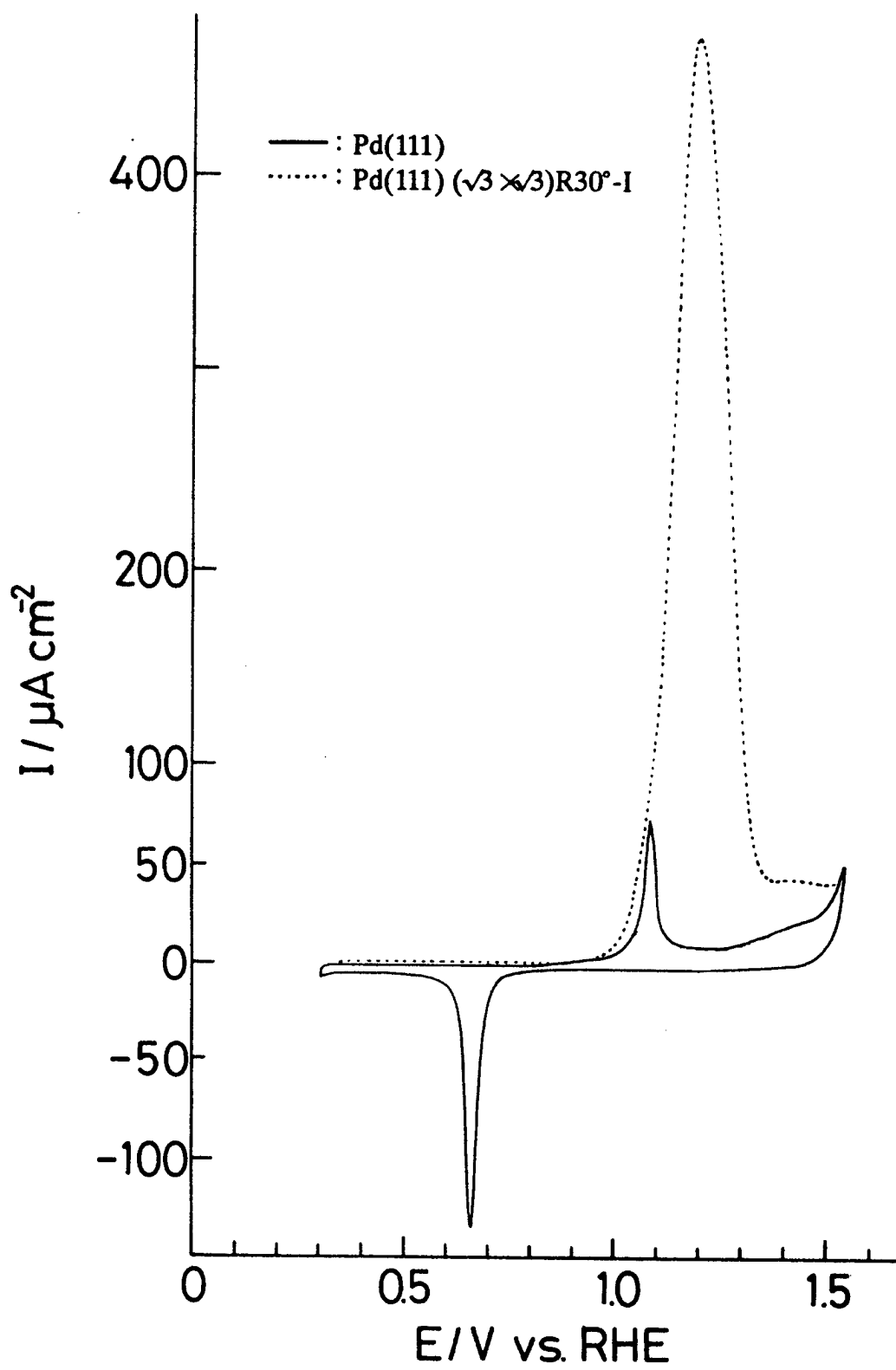
MPS wishes to acknowledge the Robert A. Welch Foundation and the Energy Resources Program of Texas A&M University. KI thanks the Ministry of Education, Science, and Culture and the ERATO-Itaya Electrochemiscopy Project, JRDC. JLS acknowledges the support of the National Science Foundation and the Office of Naval Research.

REFERENCES

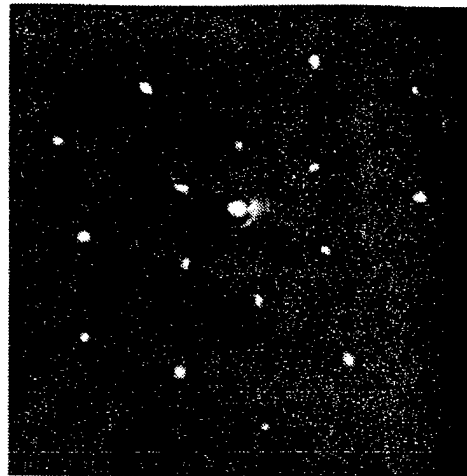
1. (a) G. Binnig, H. Rohrer, C. Gerber and E. Weibel. Phys. Rev. Lett. 50 (1983) 120.
(b) G. Binnig and H. Rohrer. Surf. Sci. 157 (1985) L373.
2. (a) M. M. Dvek, M. J. Heben, N. S. Lewis, R. M. Penner and C. F. Quate. In M. P. Soriaga, Ed. "Electrochemical Surface Science." ACS Books: Washington, D.C. 1988. (b) A. J. Bard, H. D. Abruña, C. E. Chidsey, L. R. Faulkner, S. Feldberg, K. Itaya, O. Melroy, R. W. Murray, M. D. Porter, M. P. Soriaga and H. S. White. J. Phys. Chem. 97 (1993) 7147. (c) K. Itaya. In A. T. Hubbard, Ed. "The Handbook of Surface Imaging and Visualization." CRC Press: Boca Raton, FL. 1995.
3. M. P. Soriaga. Prog. Surf. Sci. 39 (1992) 525.
4. (a) J. R. McBride and M. P. Soriaga. J. Electroanal. Chem. 303 (1989) 255. (b) J. R. McBride, J. A. Schimpf and M. P. Soriaga. J. Am. Chem. Soc. 114 (1992) 10950.
5. M. P. Soriaga, J. A. Schimpf, J. B. Abreu, A. Carrasquillo, W. Temesghen, R. J. Barriga, J.-J. Jeng, K. Sashikata and K. Itaya. Surf. Sci. 335 (1995) 273.
6. H. M. Baoming, T. E. Lister and J. L. Stickney. In A. T. Hubbard, Ed. "The Handbook of Surface Imaging and Visualization." CRC Press: Boca Raton, FL. 1995.
7. J. Clavilier. J. Electroanal. Chem. 107 (1980) 211.
8. (a) J. B. Abreu, R. J. Barriga, W. Temesghen, J. A. Schimpf and M. P. Soriaga. J. Electroanal. Chem. 381 (1995) 239. (b) J. A. Schimpf, A. Carrasquillo and M. P. Soriaga. Electrochim. Acta. 40 (1995) 1203.
9. (a) T. Meguro, M. Hamagaki, S. Modaressi, T. Hara, Y. Aoyagi, M. Ishii, Y. Yamamoto. Appl. Phys. Lett. 56 (1990) 1552. (b) P. A. Maki, D. J. Ehrlich. Appl. Phys. Lett. 55 (1989) 91.
10. Q. P. Lei, J. L. Stickney. Mat. Res. Soc. Symp. Proc. 237 (1992) 336.
11. G. A. Somorjai. "Surfaces: Chemistry in Two Dimensions." Cornell University Press: Ithaca, N.Y. (1981)

FIGURE CAPTIONS

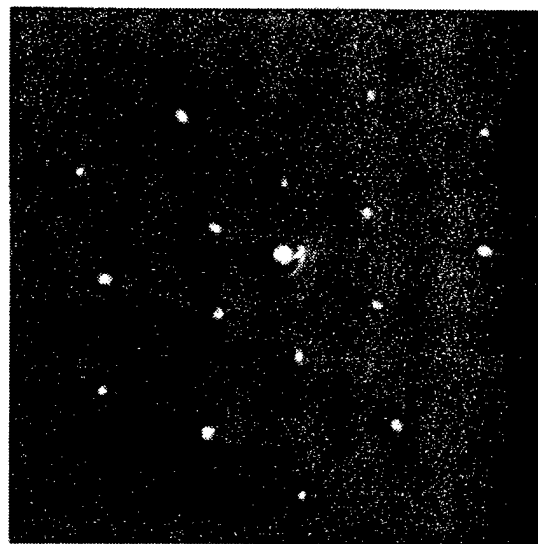
- Figure 1. Current density-vs-potential curves in the surface-oxidation region in 0.05 M H_2SO_4 for a Pd(111) facet on a single-crystal bead, clean (solid curve) and I-coated (dashed curve). Potential sweep rate, $r = 10 \text{ mV s}^{-1}$.
- Figure 2. Low-energy electron diffraction (LEED) patterns for Pd(111)- $(\sqrt{3}\times\sqrt{3})\text{R}30^\circ\text{-I}$ adlattices before and after anodic dissolution of *approximately* 30 monolayers of Pd surface atoms. Beam energy = 60 eV; beam current = $2\mu\text{A}$.
- Figure 3. *In situ* scanning tunneling microscopy images of a Pd(111)- $(\sqrt{3}\times\sqrt{3})\text{R}30^\circ\text{-I}$ facet on a single-crystal bead at various stages of adsorbate-catalyzed dissolution. M: marker; S: step.
- Figure 4. Low-energy electron diffraction (LEED) patterns: Top: Au(100)-c(2 \times 2)-Se at $\Theta = 0.5$; Bottom: Au(100)- $(3\times\sqrt{10})\text{-Se}$ at $\Theta = 0.9$. Beam energy = 62 eV ; beam current = $2 \mu\text{A}$.
- Figure 5. Scanning tunneling microscopy images: Top: Au(100)-c(2 \times 2)-Se at $\Theta = 0.5$; Bottom: Au(100)- $(3\times\sqrt{10})\text{-Se}$ at $\Theta = 0.9$.

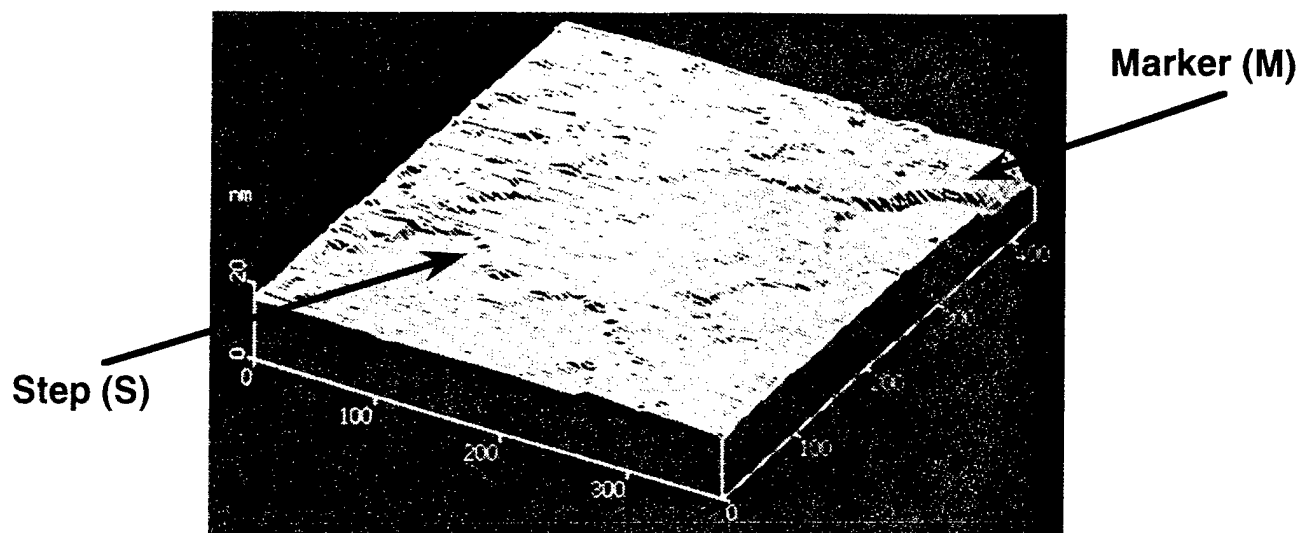


$\text{Pd}(111)-(\sqrt{3}\times\sqrt{3})\text{R}30^\circ\text{-I}$

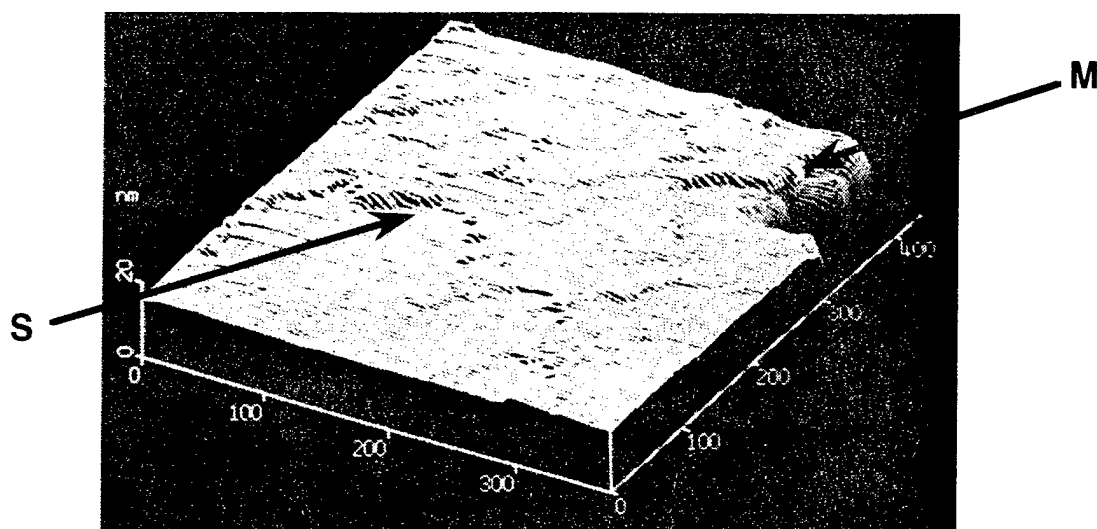


30-ML Etch

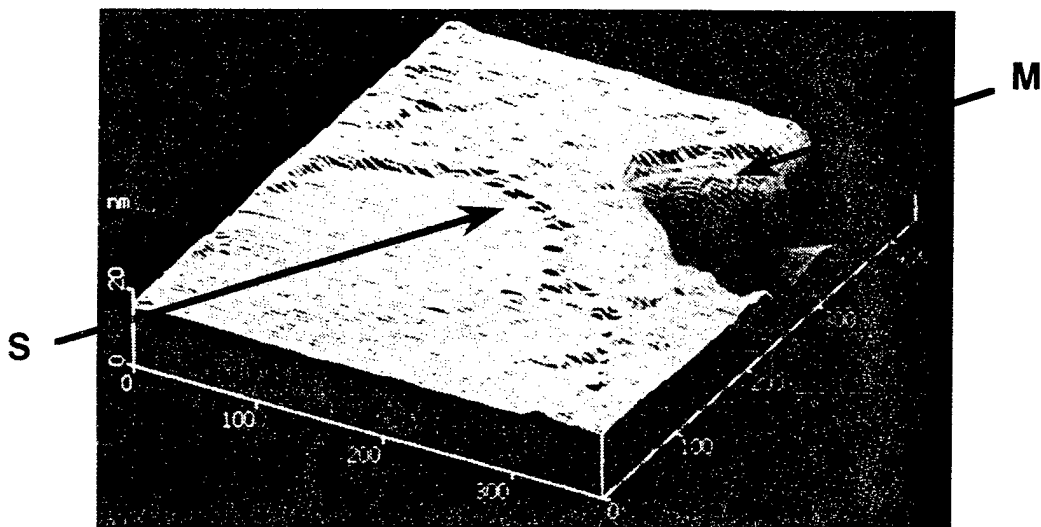


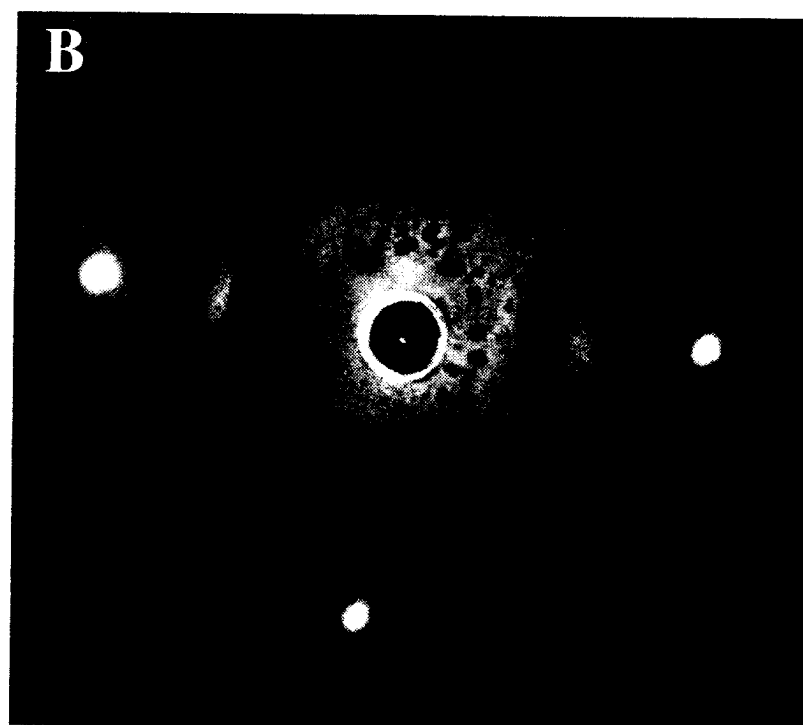
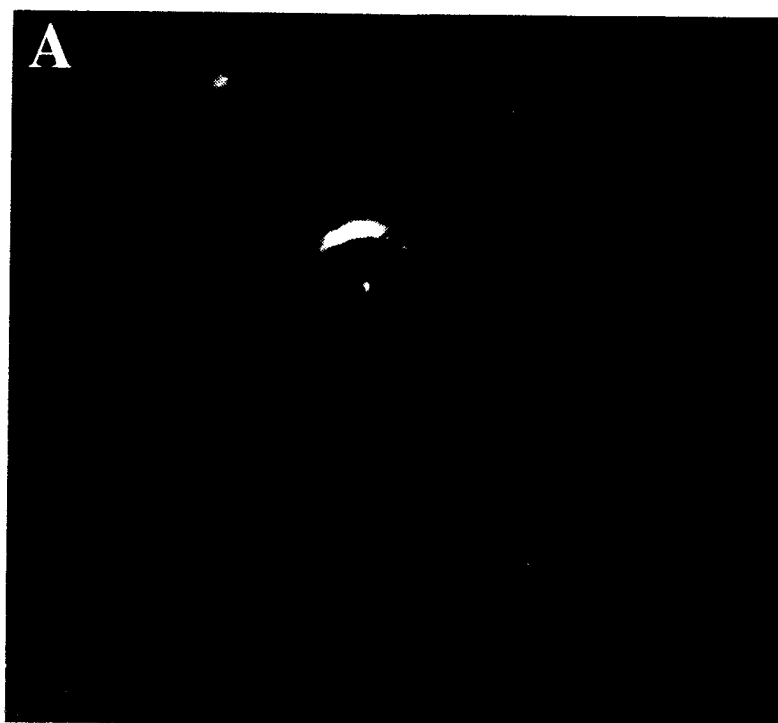


↓ 0.05 M H_2SO_4
0.9 V (RHE)/10 Minutes

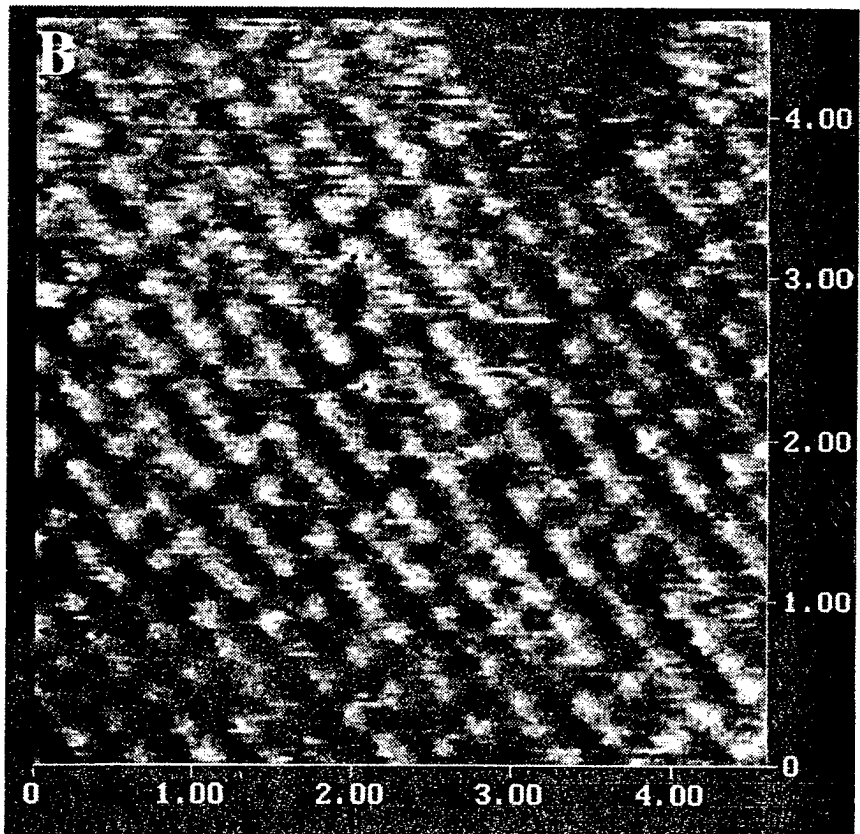
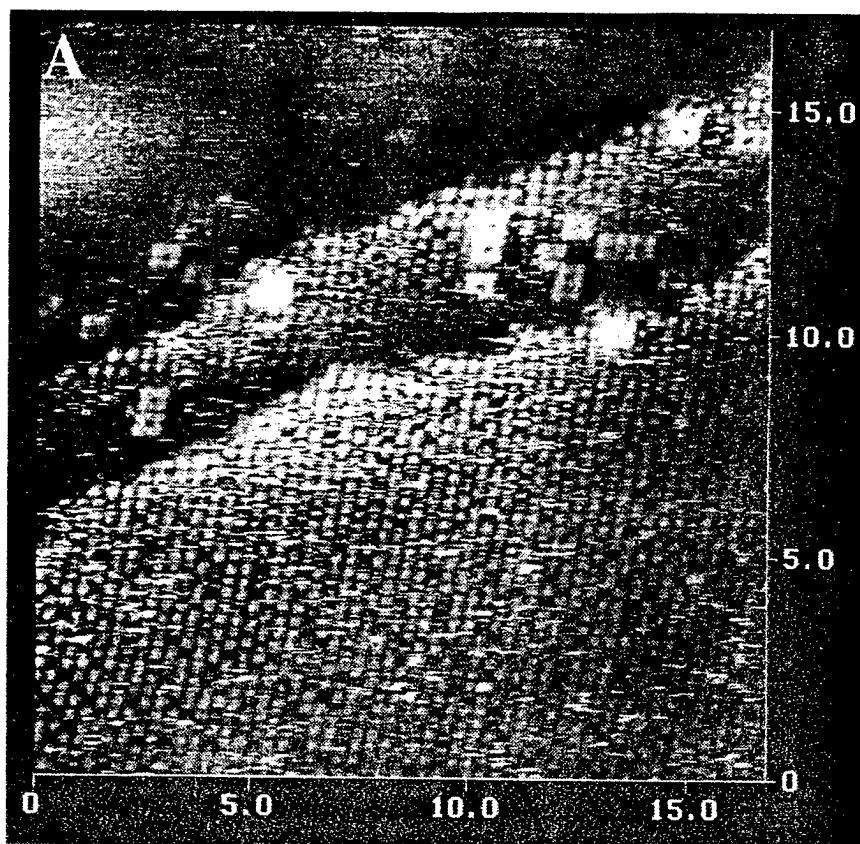


↓ 0.05 M H_2SO_4
0.9 V (RHE)/10 Minutes





Soriaga, Itaya, Stickney
"UHV-EC and *In Situ* STM...."
Figure 4.



Soriaga, Itaya, Stickney
"UHV-EC and *In Situ* STM..."
Figure 5.